Innovative Architecture of Switching Device for Expanding the Applications in Fiber to the Home (FTTH)

Mohamed Mahmoud[1] (m.mahmoud@aast.edu), **Heba A. Fayed**[1] (hebam@aast.edu),
Moustafa H. Aly[1*] (drmosaly@gmail.com),
and **A.K. AboulSeoud**[2] (Aboul_Seoud_35@yahoo.com)

[1]Arab Academy for Science, Technology and Maritime Transport, Alexandria, Egypt.
[2] Faculty of Engineering, University of Alexandria, Egypt.
[1*] OSA Member.

ABATRACT

A new device, optical cross add drop multiplexer (OXADM), is proposed and analyzed. It uses the combination concept of optical add drop multiplexer (OADM) and optical cross connect (OXC). It enables a wavelength switch while implementing add and drop functions simultaneously. So, it expands the applications in fiber to the home (FTTH) and optical core networks. A very high isolation crosstalk level (~ 60 dB) is achieved. Also, a bidirectional OXADM and N×N OXADM are proposed. Finally, a multistage OXADM is presented making some sort of wavelength buffering. To make these devices operate more efficient, tunable fiber Bragg gratings (TFBGs) switches are used to control the operation mechanism.

Keywords: magnetically tunable fiber Bragg grating, optical cross add drop multiplexer, FTTH.

1. INTRODUCTION

All optical networks have been attracting a great deal of interest in the last few years as an essential technology for the future information infrastructure [1]. This is because of their ability to provide huge data capacity, network flexibility, and reconfigurable paths for signal routing in the optical layer, thus eliminating the need for optical switches, efficient traffic rearrangement, and relaxed network management [2]. To fully exploit the huge unused bandwidth of single mode optical fibers, WDM and DWDM have been employed [3-5].

Therefore, new optical devices are required to provide additional facilities in such WDM transport networks, signal routing and network reconfiguration (i.e. the cross connect operation). OADMs are the simplest elements to introduce wavelength management capabilities by enabling the selective add and drop of optical channels [6]. An OXC is a device used in optical switching. An optical channel at one of the input ports of the OXC could be sent to any of the output ports according to the network switching requirements; as the OADMs, OXCs are a key component in the passive optical networks (PONs). Since OXCs operate in the optical domain, they can potentially accommodate terabit data streams; allow the optical network to be reconfigurable on a wavelength-by-wavelength.

FBGs have found many applications in WDM all optical networks, especially in OADM and OXC. Dynamically configurable OADMs constructed with TFBG filter will be the basis for all next generation optical networking products. In this paper, is proposed a simple, cost effective, flexible, easily upgrade and transparent configuration, using a magnetically TFBG and an OC [7-9]. A fundamental difficulty of wavelength routing is the crosstalk from neighbor inputs, which cause severe degradation in system performance.

This paper is organized as follows. Section 2 highlights the major crosstalk mechanisms and their characteristics. In Section 3**,** a new device (OXADM) is introduced. Section 4 presents a multistage OXADM that can add some sort of wavelength buffering, which we name **signal parking**. So, this multistage OXADM can be used as an optical buffer. Section 5 illustrates the upgrade of the OXADM design to get a bidirectional device. This allows the same switching

Photonics North 2011, edited by Raman Kashyap, Michel Têtu, Rafael N. Kleiman, Proc. of SPIE Vol. 8007, 80071P · © 2011 SPIE · CCC code: 0277-786X/11/$18 · doi: 10.1117/12.909221

performance in both directions. In Section 6, an N×N OXADM is created. In this new proposed N×N OXADM, we ensure any channel routed from any input port to any output port without the risk of collision with other channels. Finally, Section 7 is a conclusion.

2. EVALUATION OF INTRABAND CROSSTALK IN AN FBG-OC-BASED OPTICAL CROSS CONNECT

In all optical network introduction of OXC is limited due to presence of crosstalk. This is because the crosstalk levels are generally very high that give rise to significant signal deterioration and increased bit error rates. There are various sources of crosstalk in optical networks, due to unsatisfactory components. The definitions of optical crosstalk given vary from one literature to another, thus causing confusion. This section outlines the major crosstalk mechanisms and their characteristics. Crosstalk may be classified as either intraband (or homodyne), between signals at the same nominal wavelength or interband (or heterodyne), between signals at different wavelengths [10].

2.1 Interband Crosstalk

Interband crosstalk is due to signals wavelength different from the target channel located outside the desired channel slot, see Fig. 1.a. Interband crosstalk is non accumulative as it propagates through multiple nodes and can be reduced by employing a narrow band filter at the receiver end, similar to WDM line transmission systems. It does not produce any significant beating component during the detection process. At the receiver, it mostly acts as a random factor reducing the signal extinction ratio, since it superimposes itself on the signal in the form of a random power [10].

2.2 Intraband Crosstalk

Crosstalk elements that fall within the desired wavelength channel slot are referred to as intraband crosstalk, see Fig. 1.b,c. This is much more complex to deal with because it will accumulate while propagating through the nodes. However, it will result in a beat component, which may or may not fall within the receiver bandwidth. If it appears outside the receiver bandwidth then usually it can be ignored. It is worth mentioning that the effect of intraband crosstalk is more damaging in end-to-end transmission than the Interband crosstalk.

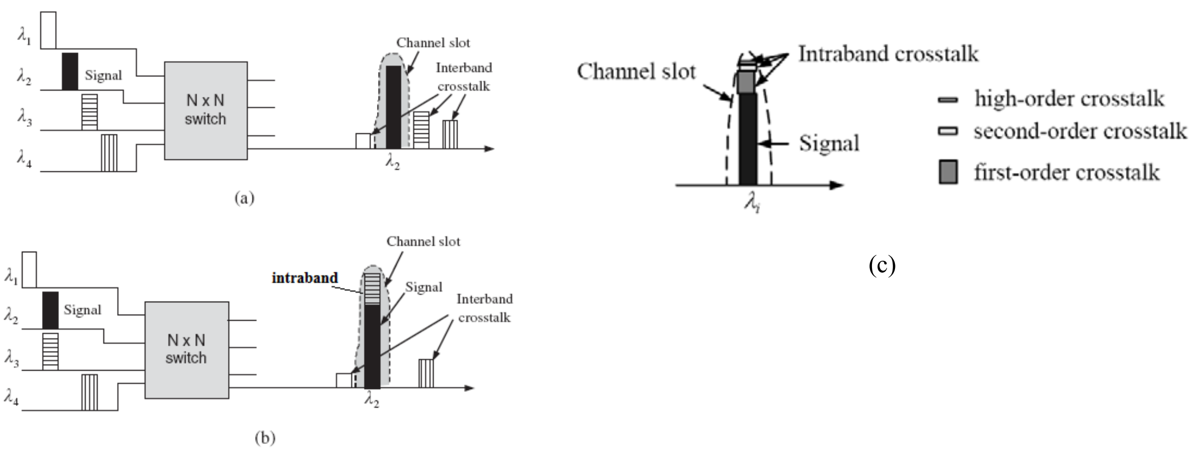

Fig. 1 Switched induced crosstalk: (a) interband, and (b,c) intraband.

The optical power at the output of a typical 2×2 cross-connect switch, with isolation x, fed with two optical signals of power P_1 and P_2, ω_1 and ω_2 the angular frequencies, φ_1 and φ_2 are phases, θ_1 and θ_2 the initial phases, and polarization p1 and p2 of both signals, respectively, is given by [10]:

$$P_0 = P_1(1-x) + P_2 x + 2\sqrt{P_1 P_2 x(1-x)} \times \cos\left[(\omega_1 - \omega_2)t + \left(\varphi_1(t) - \varphi_2(t)\right) + (\theta_1 - \theta_2)\right] p1p2 \quad (1)$$

Where the first term is the signal power, the second term is the crosstalk, and the last term is the intensity beat noise (beat). The signal waveform is corrupted by the crosstalk and the beat. The beat has a maximal value of $\pm 2\sqrt{P_1 P_2 x(1-x)}$. Purely homodyne interference effects exists: (i) the signals originated from the same source, the phase delay within coherent range, and polarization matching; (ii) the signals originated from the different sources, however with fixed wavelength difference (which is very small), same phase and fixed initial phase, and equal polarization. For this worst case, the beat term has a negative maximum - $2\sqrt{P_1 P_2 x(1-x)}$. We can write Eq. (1) as:

$$P_{worst} = P_1 + P_2 - 2\sqrt{P_1 P_2 x(1-x)} \quad (2)$$

In realistic system, purely homodyne interference effects are not expected as the interfering fields are most probably generated from different sources with polarization mismatching.

Using the general definitions, the intraband crosstalk is classified into two categories of coherent crosstalk and incoherent crosstalk. If the beat term in Eq. (2) dominates the total crosstalk, the crosstalk is denotes as coherent crosstalk (X_{CT}^{CO}). If the beat term is very small and negligible compared with the total crosstalk, the crosstalk is denoted as incoherent crosstalk (X_{CT}^{iC}). In the following section, an analytical model is established to evaluate the intraband crosstalk performance using the stage-by-stage property of FBG – OC-based OXC.

2.3 Mathematical Model of Optical Crosstalk

The intraband crosstalk is contributed by first, second- and higher order crosstalk, as shown in Fig. 1. It is dominated by the term of first-order crosstalk. For example, the level of first-order crosstalk is -40 dB, the term of second-order crosstalk is thus -80 dB, which is 40 dB smaller than the term of first-order. Here crosstalk higher than second-order is too small and not considered. Figure 2 shows a schematic structure of an N × N M-channel FBG-OC-based OXC composed of (2n-1) stages of 2 × 2 OXCs. In the example here $N = 2^n = 4$ represents the number of input/output fibers and M is the number of wavelengths per fiber.

A general 2 × 2 OXC is shown in Fig. 2. Depending on the switching states of tunable FBGs, the input signals with the same wavelengths can be routed to any of the output fibers. We designate that an arbitrary channel i is in the bar-state when it is reflected at the matching i^{th} FBG with a Bragg wavelength λ_i. In this case, the channel signal inserted in k^{th} input fiber will appear at the k^{th} output fiber. Similarly, an arbitrary channel i is in the cross-state when it passes through i^{th} FBG with a central wavelength $\lambda_i' \neq \lambda_i$. In this case, channel signal λ_i inserted from k^{th} input fiber will emerge from the j^{th} output fiber where $k \neq j$.

In Fig. 2, the thick solid lines are the paths for the main channel signals from inlet fiber 1; the dashed and short dashed lines are the first- and second-order crosstalk, (which is too small and not considered), respectively. The first-order crosstalk is mainly due to leakage paths in FBGs and OCs. Those originating from the FBG, have the same wavelength but originated from different fibers, which is classified as an incoherent crosstalk. Whereas crosstalk originated from the circulators are from the same fiber at ''bar'' state, dashed lines in Fig. 2, and from different fiber at ''cross'' state, short dashed lines in Fig. 2. Therefore, the channel in the bar state will encounters coherent and incoherent first-order crosstalk, whereas in the cross state it will only encounter incoherent crosstalk.

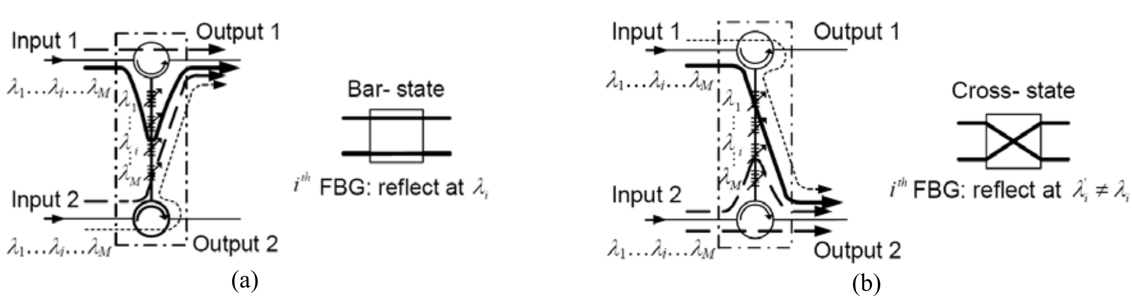

Fig. 2 Two switching states of a 2 × 2 OXC (a) bar-state and (b) cross-state.

Here we make the following assumptions: (i) all 2×2 OXC stages are in the bar-states. In a uniform FBG with very high reflectivity, the sideband crosstalk deteriorates with the increase of reflectivity at the Bragg wavelength. To improve the sideband suppression ratio, apodized fiber gratings are often used. They have a very small sideband crosstalk, which is nearly constant over a certain wavelength range. Therefore, we also assumed that (iii) the FBG's sideband profile has an average crosstalk of X_{SB} over all other channels.

In this analytical model, we assume that all 2 × 2 OXC stages are in bar-state and the FBG's sideband profile has caused an average crosstalk of X_{SB} over all other channels. The losses of devices, i.e. FBG or OC, will not be considered. Following a similar method as in the worst case optical power at the output of the first stage given as:

$$P_i^{j_{out}}(1) = P_{i_0}^{j_0}(0) + \left(P_{i_0}^{j}(0)X_{FG} + P_{i_0}^{j_0}(0)\,X_{OC}\right) - 2\sqrt{P_{i_0}^{j}(0)P_{i_0}^{j_0}(0)}\,\sqrt{X_{FG}} - 2\sqrt{P_{i_0}^{j_0}(0)P_{i_0}^{j_0}(0)}\sqrt{X_{OC}} - 2\sqrt{P_{i_0}^{j}(0)P_{i_0}^{j_0}(0)}\sqrt{X_{FG}\,X_{OC}} \quad (3)$$

where $P_{i_0}^{j_0}(0)$ and $P_{i_0}^{j}(0)$ are the input power of the signal channel i_0 from fibers j_0, and j, respectively, X_{oc} is the OC crosstalk, X_{FG} = 10 $\log_{10}$ (1 - R_{FG}) is the FBG crosstalk, R_{FG} is FBG reflectivity, $P_i^{j_{out}}(k)$ is the signal power at the output of each stage, i designates the wavelength channel (1≤ i ≤ M), j is the number of the inlet fiber (1≤ j ≤ N), k is the path stages (1≤ k ≤ 2n-1), and $P_i^{j}(0)$ is the initial input optical power of i^{th} channel from j^{th} inlet. The first and second terms are the power of signal and crosstalk, respectively. The third and forth terms are the signal-crosstalk beat noise, and the last term is the crosstalk–crosstalk beat noise. For the case of all stages being in the cross-state, all X_{FG} is simply replaced by X_{SB} in Eq. (3). For simplicity, we have assumed that all channels have the same initial input power P(0). Thus, at the output of the first stage the optical power is simplified as:

$$P(1) = P(0)\left[1 + X_{FG} + X_{OC} - 2\left(\sqrt{X_{FG}} + \sqrt{X_{OC}} + \sqrt{X_{FG}\,X_{OC}}\right)\right] \quad (4)$$

The output power at k^{th} stage is given as

$$P(k) = P(k-1)\left[1 + X_{FG} + X_{OC} - 2\left(\sqrt{X_{FG}} + \sqrt{X_{OC}} + \sqrt{X_{FG}\,X_{OC}}\right)\right] \quad (5)$$

At the output of an N× N FBG–OC-based OXC, the coherent crosstalk X_{CT}^{CO} and the incoherent crosstalk X_{CT}^{iC} are given as:

$$X_{CT}^{CO} = 10\log_{10}\left|\left[1 + X_{FG} + X_{OC} - 2\left(\sqrt{X_{FG}} + \sqrt{X_{OC}} + \sqrt{X_{FG}\,X_{OC}}\right)\right]^{2n-1} - 1\right| \quad (6)$$

$$X_{CT}^{iC} = 10\log_{10}[[1 + X_{FG} + X_{OC}]^{2n-1} - 1] \quad (7)$$

$$= 10\log_{10}[\ (2n-1)(X_{FG} + X_{OC}) + \frac{(2n-1)(2n-2)}{2(X_{FG}+X_{OC})^2} + \cdots + \frac{n!}{(n-k)!k!}\,(X_{FG} + X_{OC})^{2(n-k)-1} + \ \ldots + ((X_{FG} + X_{OC})^{2n-1}\ ] \quad (8)$$

Note that both crosstalk depend on network parameter n and component crosstalk X_{OC} and X_{FG}. They are completely independent of the number of wavelength channels per fiber M and the input optical power level P(0). Expanding or by Taylor series, at the output of N × N OXC, the number of first-order and second-order crosstalk contributions can be easily obtained.

3. DESCRIPTION OF FIRST STRUCTURE OXADM AND ITS IMPLEMENTATION

The first structure to be presented, OXADM, is shown in Fig. 3. This structure consists of three TFBGs and two MOCs. The TFBG3 is used to rout the input signal (input 1 or input 2) to the required output port (output 1 or output 2). The other TFBGs 1, 2 are used to add and drop signals.

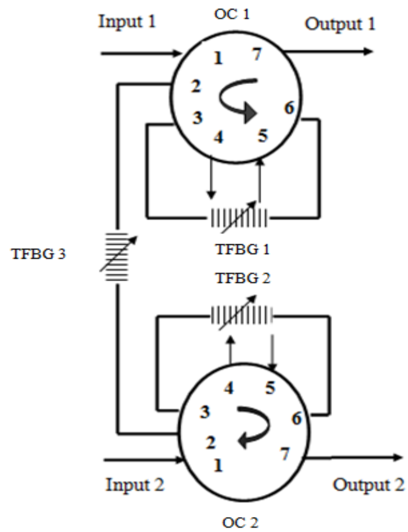

Fig. 3 2×2 OXADM using MOC and TFBGs.

For example, an input signal, placed at input 1 (port 1 OC1), is obtained through lasers spectra and are composed of three wavelengths; λ_1 = 1549.9 nm (193.56 THz), λ_2 = 1550.7 nm (193.46 THz) and λ_3 = 1551.5 nm (193.36 THz), separated by 0.8 nm (100 GHz) as the ITU grid [2]. The TFBG3 λ_M is used as a tunable optical filter and in this example, it was tuned with a central wavelength of λ_2 =1550.7 nm (193.46 THz). Another input signal is placed at input 2 (port 1 OC2), with the same wavelength, λ_2 =1550.7 nm. This is shown as the most extreme case to demonstrate the cross talk on the output signals. Let $\lambda_{TFBG1} = \lambda_2$ (to add and drop signal) and $\lambda_{TFBG2} = \lambda_2$ (to drop λ_2 from port 4 in OC1 and OC2, also add another λ_2 from port 5 in OC1 and OC2).

3.1 OXADM1 Simulation Results

The simulation results show the switching states of the TFBG including bar and cross-states and simultaneous selective channel switching sending each desired channel to any given port. The FBGs are electrically controlled and act as wavelength selective filters that properly route the input signals to the desired output port. Any wavelength λ_1; . . λ_N can be applied at the input ports of this configuration. Collision between channels of the same wavelength is avoided by tuning the grating in pairs; for example, if λ_1 at input 1(OC1) is routed to output 1, the signal λ_1 at input 2 is automatically routed to output 2 when TFBG3 adjusted at λ_1.

In order to evaluate the performance of this OXADM1, laser sources with high power output provided the defined channels an input signal, placed at input 1 (port 1 OC1), are composed of three wavelengths (λ_1, λ_2, and λ_3) where λ_1 = 1549.9 nm, λ_2 = 1550.7 nm and λ_3 = 1551.5 nm. In this simulation, λ_{TFBG3} is adjusted to equal λ_2. Due to this configuration, λ_2 is reflected from TFBG3 to port 2 in OC1, then it is sent to port 3, λ_{TFBG1} is set to equal λ_2, TFBG1 will reflect λ_2 to port 3 in OC1 and then port 4 which is the dropped signal. The added signal will be input from port 5 then to port 6 and out from port 7 which is output 1. This shows an example of a bar state switching with add and drop wavelength. Another input signal, placed at input 2 (port 1 OC2), with the same wavelength, λ_2, because $\lambda_{TFBG3} = \lambda_2$, λ_1 and λ_3 will pass from TFBG3 and sent to port 2 in OC2. Also, λ_2 (input 2 port 1 in OC2) is reflected from TFBG3 to port 2 in OC2, then λ_1, λ_2, and λ_3 are sent to port 3 in OC2, λ_{TFBG2} is also set to equal λ_2 = 1550.7 nm (193.46 THz). TFBG2 will reflect λ_2 to port 4 (in OC2) where λ_2 is dropped; another λ_2 is added through port 5 (in OC2). λ_1, λ_3 and the added λ_2 will transmit to port 6 in OC2 and then port 7 which is output 2. This shows an example of a cross state switching (λ_1 and λ_3 inserted from input 1 to output 2), and bar state switching for λ_2 with add and drop wavelength capabilities.

Figure 4 shows the output 1 from port 7 in OC1, due to the bar state configuration for λ_2. As shown in Fig. 4, the homodyne crosstalk occurs at λ_2. The first crosstalk is due to the non-complete reflection of the TFBG1. Because of this reason, the drop signal which must be completely reflected from TFBG1, a small power from this signal transmits to port

5 then to port 6 finally to port 7 which is the output 1. The amplitude of this crosstalk is -32.94 which is acceptable. The second crosstalk is due to non-complete reflection of TFBG3 and TFBG1. When λ_2 (from input 2) is reflected from TFBG3, a small power from λ_2 is transmitted to port 2 in OC1. This signal also is transmitted from TFBG1 and causes homodyne crosstalk -64.48 dBm. The homodyne crosstalk isolation level is shown to be 31.951 dBm, which one can improve it in the next multistage OXADM design. Also, a heterodyne crosstalk results from the reflection of the TFBG3 of a small power from the input signals λ_1 and λ_3 is shown. As can be shown, the heterodyne crosstalk isolation level is very small less than (-118 dBm) which can be easily neglected.

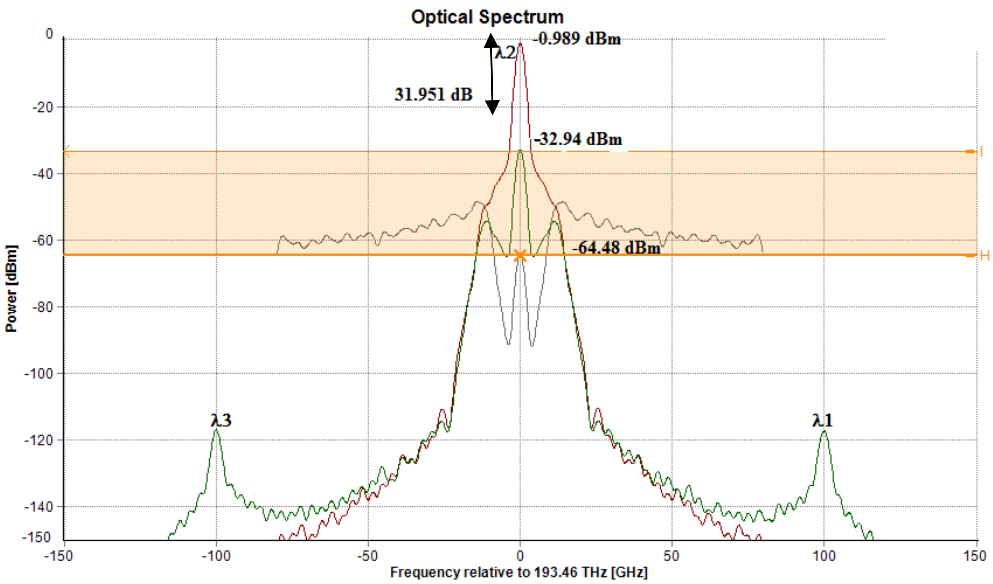

Fig. 4 Output 1 from OC1 when TFBG3 tuned at 193.46 THz for OXADM1.

Figure 5 shows the drop signal from port 4 in OC1. It can be shown that λ_2 is dropped, because TFBG1 is tuned at λ_2. Also, λ_2 is attenuated due to passing by OC and TFBGs by -1.401 dBm.

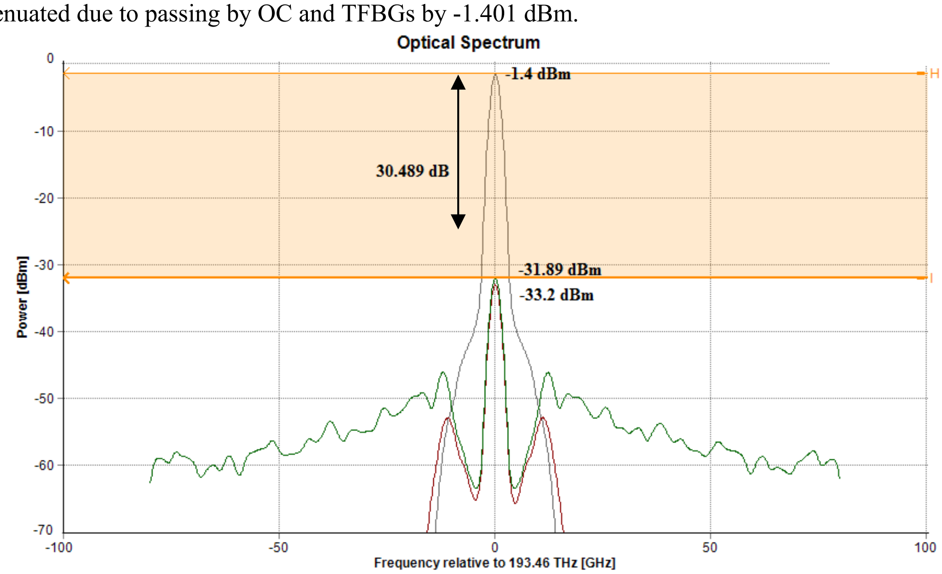

Fig. 5 Drop signal from port 4 at OC1 for OXADM1.

Figure 6 shows the output 2 from port 7 in OC2. It can be shown that λ_1, λ_2 and λ_3 suffer from small attenuation; λ_2 due to the incomplete reflection from TFBG2 and λ_1 and λ_3 due to incomplete transmit through TFBG3. Also, both λ_1 and λ_3

pass by TFBG2. While λ_2 is a new added signal but also suffers from small attenuation due to passing through a circulator.

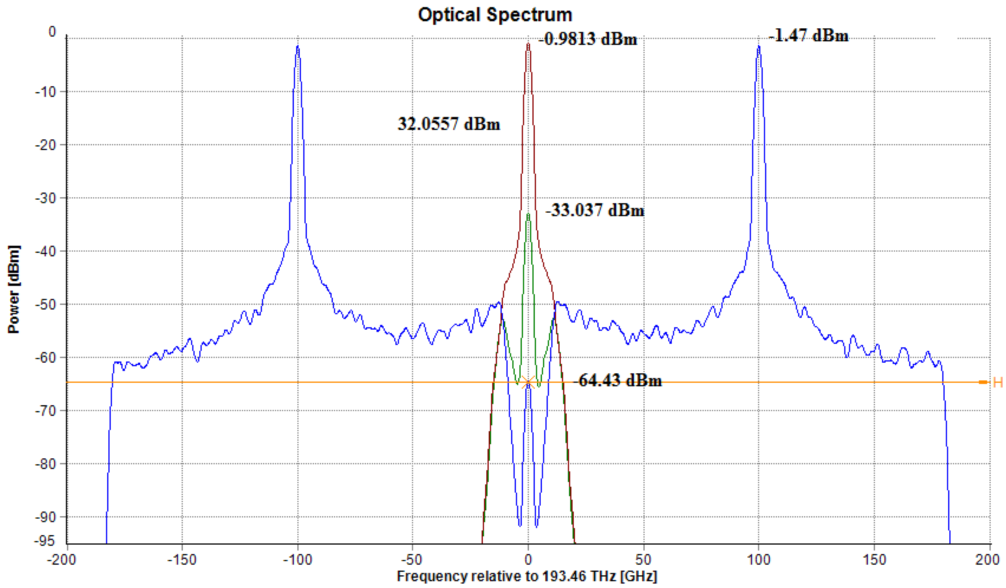

Fig. 6 Output 2 from port 7 in OC2 for OXADM.

Table 1 illustrates the comparison between the OXC + OADM (Cascaded) and OXADM. It is clear, that, the OXADM is better than OXC + OADM in dropped signal. Because OXADM uses two OCs instead of six OCs, so, the insertion loss will be reduced. Moreover, using two-circulator device is much more economical than the six-circulator device and is easier in design.

Table 5.3 Comparison between OADM + OXC and OXADM.

		OADM + OXC	OXADM
Drop 1	Amplitude of λ_2 (dBm)	-2.289	-1.4
	Amplitude of homodyne crosstalk (dBm)	-31.89	-31.89
	Amplitude of the second homodyne crosstalk (dBm)	-33.52	-33.2009
	Crosstalk isolation levels (dB)	29.601	30.489
Output 1	Amplitude of λ_2 (dBm)	-0.989	-0.989
	Amplitude of homodyne crosstalk (dBm)	-32.38	-32.94
	Amplitude of the second homodyne crosstalk (dBm)	-64.607	-64.48
	Crosstalk isolation levels (dB)	31.391	31.951
Drop 2	Amplitude of λ_2 (dBm)	-2.28	-1.4
	Amplitude of homodyne crosstalk(dBm)	-31.96	-31.68
	Amplitude of the second homodyne crosstalk(dB)	33.61	33.061
	Crosstalk isolation levels(dB)	29.68	30.28
Output 2	Amplitude of λ_2(dBm)	-0.987	-0.9813
	Amplitude of λ_1 , λ_3(dBm)	-2.242	-1.47
	Amplitude of homodyne crosstalk(dBm)	-33.27	-33.037
	Amplitude of the second homodyne crosstalk(dBm)	-65.046	-64.43
	Crosstalk isolation levels(dB)	32.283	32.05

4. A MULTISTAGE STRUCTURE OF 2×2 OXADM AND ITS IMPLEMENTATION

In this Section one can be achieved better isolation levels 50 dB using the same design as in Section 3 but using a TFBG with higher rejection ratio (50% instated of 30%). The multistage OXADM, which is built as depicted in Fig. 7 is composed of four multiport optical circulators and six TFBGs. At first, *N* multiplexed wavelengths are fed to the TFBG through the circulator, and then the filtered signal is reflected and goes back to the circulator and then the signal passes by the add/drop port (at ports 4-5 in the circulator). The optical switch allows the selection of the add/drop operation by removing and adding the channel or passing through operation, where the removed channel can be added again.

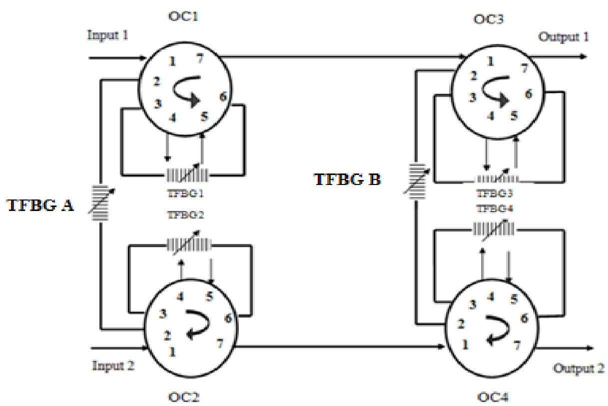

Fig. 7 Multistage structure 2×2 OXADM.

5. OXADM BI-DIRECTIONALITY

As in the previous architectures, additional FBGs can be used to control more optical channels at the same time. These architectures have the possibility of being upgraded to ensure bi-directionality, i.e., allowing the same switching performance in both directions. This configuration is illustrated in Fig. 8 and it demands only the addition of four multiport optical circulators and eight tunable gratings. The conjugation of these architectures with active devices is such as semiconductor optical amplifier.

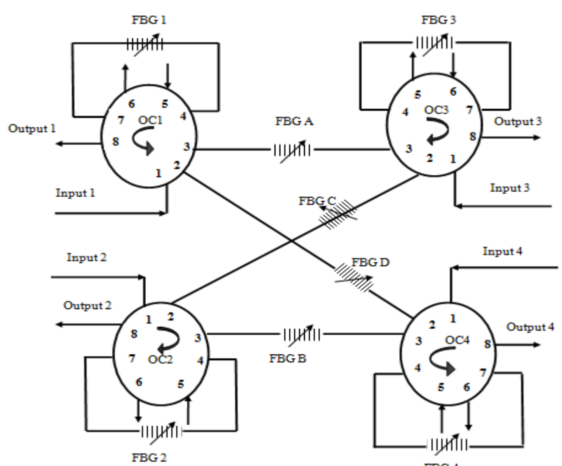

Fig. 8 Proposed architecture of bi-directional OXADM.

6. N×N OXADM SCALABILITY CAPABILITIES

Concerning N×N OXADM scalability, this device offers many possibilities, one of which is depicted in Fig. 9 which shows a 4×4 OXADM constructed with 6 elementary 2×2 OXADM1. Any channels present at the input ports are properly routed to one of the output fibers without the risk of collision with other channels using the same wavelength.

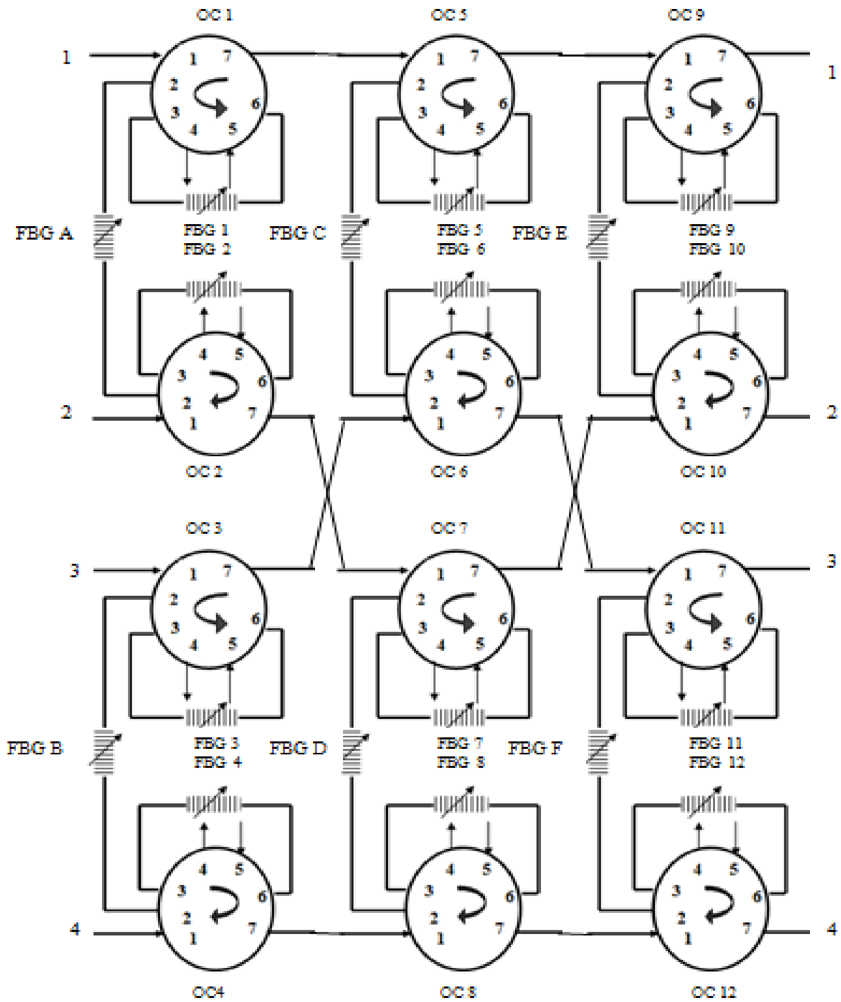

Fig. 9 N×N OXADM.

In terms of insertion losses, our structure has worse performance due to the increased number of optical circulators and FBGs. These losses can be reduced
using multi-port optical circulators [10].

7. CONCLUSION

The nature of internet traffic inspires us to look for technologies offering enormous bandwidth. The only way to cope with this bandwidth demand is optical networks. But, a shortage in the optical devices, systems and sub-systems exist. This paper aims to propose some solutions for optical devices, which will help in achieving our goal for all optical networks that will carry the required bandwidth. The solutions include the development of a new design of multifunction optical switch combining the two functions; OXC and OADM into a single device called optical cross add drop multiplexer (OXADM). Also, an enhancement of the OXADM for a better isolation crosstalk level is achieved. A scalable tunable OXADM based on FBG-OC with the possibility of bi-directionality is proposed and demonstrated. The operation of the OXADM has been simulated by VPI software and its performance evaluated. Good results have been obtained in terms of crosstalk levels. The worst crosstalk isolation level obtained was 30.4 dB and the maximum insertion loss was -2.28 dBm. The Interband and intraband crosstalk isolation level obtained with this OXADM design and simultaneously using TFBGs was proposed. When comparing these results with previously published work on other structures our crosstalk levels are acceptable. Using the multi-port optical circulators lead to improved crosstalk results.

REFERENCES

[1] Mohamed M. Ali, Moustafa H. Aly and Hossam M. H. Shalaby, "Wavelength Reservation and Traffic Loading in Optical Burst Switching Network Design: A Comparison Between Different Techniques," Proceeding of the 3rd Saudi Technical Conference, Reyadh, Saudi Arabia, vol. II, pp. 272-279, Dec. 11-14, 2004.

[2] Wael Hosny, Mohamed M. Ali, Moustafa H. Aly and El-Sayed A. El-Badawy, "Effect of Link Bandwidth, Number of Channels and Traffic Load on Designing Optical Burst Switching Networks," Proceeding of the 18th International Conference on Computer: Theory & Applications, ICCTA 2008, Alexandria, Egypt, pp. 47-51, Oct. 11-13, 2008.

[3] Wael Hosny, Mohamed M. Ali, Moustafa H. Aly and El-Sayed A. El-Badawy, "New Optical Parameters Dependent Metric for Effect of Link Open Shortest Path First Routing Protocol for Optical Burst Switching Networks," Proceeding of the 6th International Conference on Wireless Optical Communications Networks WOCN2009, Cairo, Egypt, ISBN 978-1-4244-3474-9 ©2009 IEEE, Paper S15-7, April 28-30, 2009.

[4] Mohamed M. Ali, Moustafa H. Aly, El-Sayed A. El-Badawy and Wael Hosny, "Optical Parameters and Link Delay Dependent Routing Metric for OBS Networks," Proceeding of the 6th International Symposium on High Capacity Optical Networks and Enabling Technologies HONET'09, 978-1-4244-5995-7/09/$26.00©2009 IEEE, pp. 254-260, Alexandria, Egypt, Dec. 28-30, 2009.

[5] Mohamed M. Ali, Wael Hosny, El-Sayed A. El-Badawy and Moustafa H. Aly, "Unequal Load Balance Routing for OBS Networks Based on Optical Parameters Dependent Metric," Proceeding of the 27th National Radio Science Conference, NRSC'2010, Menouf, Egypt, pp. D8 (1-11), March 16-18, 2010.

[6] Moustafa H. Aly and Heba A. Fayed, "Compensating Bragg Wavelength Drift due to Temperature and Pressure by Applying an Artificial Strain", Proceeding of the 3rd Saudi Technical Conference, vol. IV, pp. 105-110, Reyadh, Saudi Arabia, Dec. 11-14, 2004.

[7] A.K. Aboul Seoud, Moustafa H. Aly, and Heba A. Fayed, "Tunable optical buffer using a fiber Bragg grating array and a widely tunable wavelength converter" Photonics North , Canada, Proc. of SPIE Vol. 7386, pp. 73861Y.1-73861Y.8., 2009.

[8] Heba A. Fayed, Mohamed Mahmoud, A.K. Aboul Seoud, and Moustafa H. Aly, "Magnetically Tunable Fiber Bragg Grating Supported by Guiding Mechanism System" Photonics North, Canada, Proc. of SPIE Vol. 7750, pp. 77501Z.1- 77501Z.11, 2010.

[9] Heba A. Fayed, Mohamed Mahmoud, A.K. Aboul Seoud, and Moustafa H. Aly, "A Wide Range Tunable Fiber Bragg GratingUsing Fast Changeable Electromagnetic Force" Photonics North, Canada, Proc. of SPIE Vol. 7750, pp. 77501R.1- 77501R.10, 2010.

[10] T. Gyselings, G. Morthier, and R. Baets, "Crosstalk analysis in multiwavelength optical cross connects", J. Lightwave Technol., vol. 17, no. 8, pp. 1273-1283, Aug. 1999.